

A Monolithic InGaP/GaAs HBT VCO for 5GHz Wireless Applications*

Chen Liqiang[†], Zhang Jian, Li Zhiqiang, Chen Pufeng, and Zhang Haiying

(Institute of Microelectronics, Chinese Academy of Sciences, Beijing 100029, China)

Abstract: A monolithic voltage controlled oscillator (VCO) based on negative resistance principle is presented utilizing commercially available InGaP/GaAs hetero-junction bipolar transistor (HBT) technology. This VCO is designed for 5GHz-band wireless applications. Except for bypass and decoupled capacitors, no external component is needed for real application. Its measured output frequency range is from 4.17 to 4.56GHz, which is very close to the simulation one. And the phase noise at an offset frequency of 1MHz is -112dBc/Hz . The VCO core dissipates 15.5mW from a 3.3V supply, and the output power ranges from 0 to 2dBm. To compare with other oscillators, the figure of merit is calculated, which is about -173.2dBc/Hz . Meanwhile, the principle and design method of negative resistance oscillator are also discussed.

Keywords: VCO; MMIC; wireless communication; InGaP/GaAs HBT

EEACC: 1130B; 1230B

CLC number: TN752.5

Document code: A

Article ID: 0253-4177(2007)06-0823-06

1 Introduction

Oscillators have become essential components since Edwin Armstrong discovered the superhetrodyne principle. In this application^[1], an oscillator feeds sinusoidal signals to a nonlinear mixing element to effect frequency translation by multiplying the oscillator's signals with other input signals. Today, voltage controlled oscillator (VCO) is one of the most important circuits in wireless transceivers as a part of frequency synthesizers, which are commonly used in wireless systems^[2~4] and other communication systems which must tune across a band of frequencies.

Recently, the increasing demand for high speed data communication makes the use of 5GHz wireless applications more widely, such as IEEE802.11a and HIPERLAN, which can enable the speed of data transmission up to 54Mbps. Monolithic microwave integrated circuits (MMIC) VCOs are very important building blocks in the implementation of these modern communication systems. Differing from some oth-

er reported 5GHz works^[5~9], the InGaP/GaAs hetero-junction bipolar transistor (HBT) technology is utilized due to the inherent low noise performance and high frequency characteristics. Thus the complexity of circuit topology could be simplified properly while the performance is still acceptable. It helps in achieving higher yield and smaller chip size.

The VCO described in this paper is a negative resistance oscillator made by InGaP/GaAs HBT with an emitter width of $2\mu\text{m}$, cut-off frequency (f_T) of 30GHz and maximum oscillation frequency (f_{max}) of 90GHz at 6mA, 3.5V. To achieve a fully integrated VCO, the varactor for frequency tuning must be realized with on-chip devices. Thus, the base-collector capacitor of HBT is utilized as the tuning element. The tuning range of the base-collector junction capacitance has to be taken into account to get the desired tuning range of VCO. As a result, the achieved VCO has a tuning range of more than 300MHz and phase noise of -112dBc/Hz at an offset frequency of 1MHz. To compare with other VCOs, the figure of merit for the VCO is also calculated, which is about -173.2dBc/Hz .

* Project supported by the National Natural Science Foundation of China (No.60276021) and the State Key Development Program for Basic Research of China (No. G2002CB311901)

[†] Corresponding author. Email: chenliqiang@ime.ac.cn

Received 25 December 2006, revised manuscript received 22 January 2007

©2007 Chinese Institute of Electronics

2 Principle of negative resistance oscillator

Figure 1 shows the basic principle of one-port negative resistance oscillator^[10]. The input impedance of the active device is $Z_{IN} = R_{IN} + jX_{IN}$. The active device is terminated with a passive load whose impedance is $Z_L = R_L + jX_L$. Applying Kirchhoff's voltage law yields:

$$(Z_{IN} + Z_L)I = 0 \quad (1)$$

The following conditions must be satisfied when the oscillation occurs, i. e. the RF current I is none-zero.

$$R_L + R_{IN} = 0, X_L + X_{IN} = 0 \quad (2)$$

Since the load is passive, $R_L > 0$ and thus $R_{IN} < 0$. Thus, a negative resistance implies a power generation while a positive resistance implies power dissipation. The condition that $X_L = -X_{IN}$ determines the frequency of oscillation. The process of oscillation depends on the nonlinear behavior of the input impedance Z_{IN} as follow. Initially, it is necessary for the overall circuit to be unstable at the designed frequency, so

$$R_{IN}(I, \omega) + R_L < 0 \quad (3)$$

To satisfy Eq. (3), a value of $R_L = |R_{IN}/3|$ is commonly used in practical oscillator design. Any transient excitation or noise could cause oscillation to build at the frequency ω . As I increases, the value of R_{IN} becomes less negative until the value of $R_L + R_{IN} = 0$. The oscillator is now operating in a stable state.

3 Circuit design

The VCO we built is a kind of LC negative resistance oscillator based on the principle in Section 2. Additionally a buffer stage is used not only to provide better isolation, which could improve the frequency pulling effect caused by the varia-

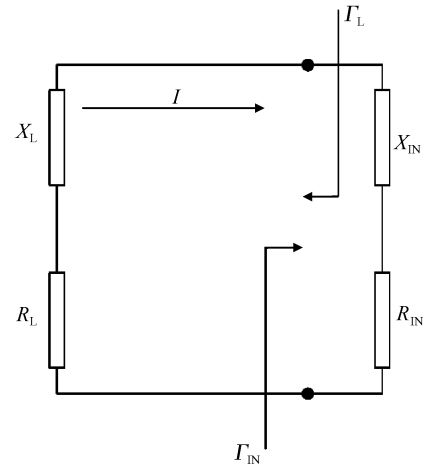


Fig. 1 Principle of negative resistance oscillator

tions of the load impedance, but also to increase the output power as needed. The overall block diagram of the VCO is illustrated in Fig. 2. A basic circuit for the tuning of parallel resonant circuits by means of varactor diodes is illustrated in Fig. 3. In this diagram, C_D is the decoupling capacitor and R_B is a bias resistor as well as a decoupling resistor. C_P is the parasitic shunt capacitance mainly in inductor L and the two varactor diodes, C_{VAR1} and C_{VAR2} . C_P are not the real components in the design library, but this parasitic capacitance does exist in the resonant circuit and impact the frequency tuning range of the VCO, as shown in Eq. (4). Therefore this impact must be taken into account in order to get relatively accurate frequency predication. The ratio of the highest oscillating frequency f_{OSC_max} to the lowest oscillating frequency f_{OSC_min} is shown in Eq. (4).

$$\frac{f_{OSC_max}}{f_{OSC_min}} = \left[\frac{1 + \frac{C_{max}}{C_P(1 + C_{max}/C_{VAR1})}}{1 + \frac{C_{max}}{C_P(C_{max}/C_{min} + C_{max}/C_{VAR1})}} \right]^{1/2} \quad (4)$$

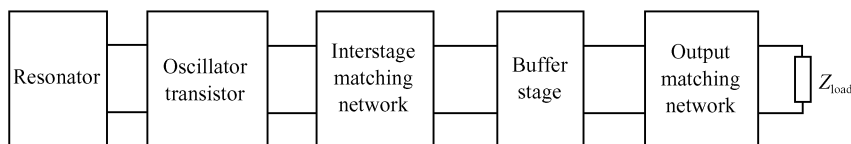


Fig. 2 Block diagram of the VCO

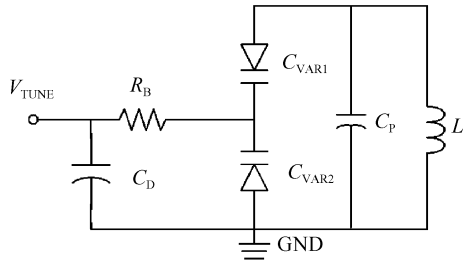


Fig. 3 Parallel-resonant circuit with two varactor diodes

where C_{\max} and C_{\min} are the maximum and minimum capacitance of the varactor diode $C_{\text{VAR}2}$, respectively^[11].

In Fig. 3, the resonator is tuned by two varactor diodes, which are connected in parallel via the inductor for tuning purposes. But the two diodes are series-connected in opposition for high-frequency signals. This arrangement has the advantage that the capacitance shift caused by the AC modulation acts in opposite directions in these diodes, and therefore, cancels itself. To achieve a fully integrated VCO, the varactor diodes must be realized with on-chip devices. After some analysis and simulation, the base-collector junction is selected to act the role of varactor diode under the consideration for frequency tuning range and linearity. Several HBTs are connected in parallel to get the desired capacitance due to the small capacitance of one single base-collector junction, as shown in Fig. 4

Besides frequency tuning range, another important parameter of the VCO is the phase noise. A higher quality factor (Q) of the tank helps in suppressing the phase noise as shown by Leeson's equation^[12] below:

$$L(\Delta\omega) = 10\lg\left[\frac{2FkT}{P_{\text{signal}}}\left(\frac{\omega_0}{2\Delta\omega Q}\right)^2\right] \quad (5)$$

Here, $L(\Delta\omega)$ is the phase noise at offset frequency $\Delta\omega$ from the carrier at ω_0 , P_{signal} is the VCO signal power at the tank, k is the Boltzman constant, T is the temperature, and F is a factor representing device noise. As we all know, the Q of a varactor is much higher than that of an inductor. Thus the inductor that has the highest Q at 4.3GHz is chosen for low phase noise since the Q of the tank is mainly determined by the Q of the inductor. In this InGaP/GaAs HBT foundry process, various types of inductors (various width,

gap, and inner diameter) are offered. The 3-turn inductor giving maximum Q of 16 at 4.3GHz is chosen for the resonator inductor.

After the inductor and varactor diodes are selected properly under the formula $f = \frac{1}{2\pi\sqrt{LC}}$, the whole resonator is done. Now the negative resistance described in Section 2 is needed to compensate the power dissipation in the resonator. In this design, the common-base for HBT is preferred due to the ease of tuning that it provides and an inductor is added to the base to provide positive feedback, which increases the negative resistance of the transistor even further. But it is not always the case that larger inductors make the oscillating easier and the whole circuit better. In spite of the extra chip size caused by the larger on-chip inductors, we found that larger feedback inductance made the impedance matching more difficult during our simulation. Thus we used an inductor of 0.8nH, which is a tradeoff between negative resistance, impedance matching and chip size. The phase noise also depends on the currents passing through the core HBTs because the current gain and shot noise of HBT transistors strongly depend on collector currents, so HBT collector current I_C should be chosen at the optimal current for low phase noise.

Until now we have got the main parts of the VCO, but it is not suitable for practical application because the bad isolation of the output may cause many negative influences on the oscillator. For example, a common problem is the frequency change exhibited by a VCO in response to varying load conditions, also known as frequency pulling. A change in impedance seen by the VCO output can induce changes in the DC voltages across junctions of the VCO's active device. The changes would affect the output frequency and phase noise performance, or even make the oscillator out of work. Another frequency-pulling phenomenon is sometimes referred to injection locking or injection pulling. It concerns the effect of an interfering signal that is very near the operating frequency of the VCO. When the amplitude of an interferer at the VCO output port is sufficient enough, it could cause the VCO to shift its oscillation frequency to match the interfering frequency^[13]. An effective way to solve these problems is to add a

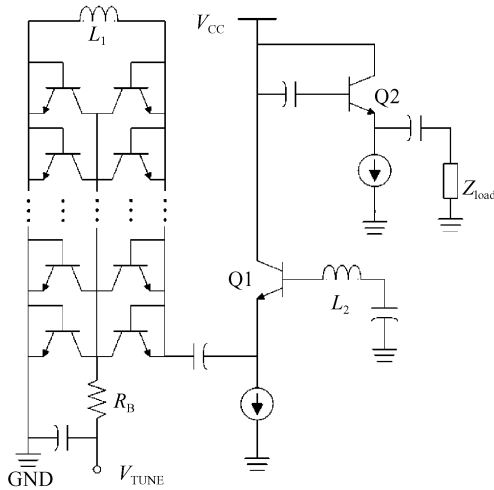


Fig. 4 Schematic of the InGaP/GaAs HBT VCO

buffer amplifier stage between the oscillator core HBT and the load. In this design, the buffer stage is implemented with emitter follower because of its high input impedance and wide bandwidth.

The entire InGaP/GaAs HBT VCO circuit was designed in Agilent Advanced Design System (ADS) and simulated by Harmonic Balance in ADS. The schematic is shown in Fig. 4, in which the bias and impedance matching networks are omitted. The power supply voltage V_{CC} is 3.3V and the tuning voltage V_{TUNE} is from 0 to 3V. The simulated frequency range is from 4.11 to 4.59GHz.

The designed VCO has been fabricated by $2\mu\text{m}$ InGaP/GaAs HBT foundry process. The large signal model of the transistor was performed using Vertical Bipolar Inter-Company (VBIC) model. One-finger $2\mu\text{m} \times 10\mu\text{m}$ HBTs were used as oscillator core transistors. This device shows a cut-off frequency of 30GHz and a maximum oscillation frequency of 90GHz. Turn-on voltage of HBT is about 1.20V. The technology provides a SiN_x metal-insulator-metal (MIM) capacitor with $600\text{pF}/\text{mm}^2$, a $50/\square$ NiCr resistor and two inter-connecting metal, of which thickness are $1.5\mu\text{m}$ and $4\mu\text{m}$, respectively. The whole circuit is passivated with polyimide. The wafer is thinned to $95\mu\text{m}$ with backside via holes. Figure 5 shows the microphotograph of the fabricated VCO.

4 Results

The test was performed with chip-on-board

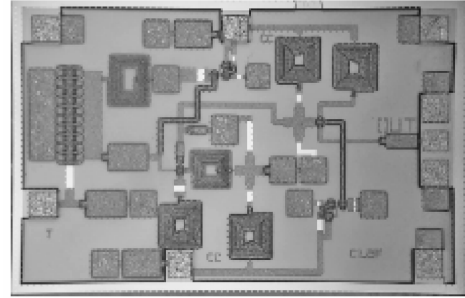


Fig. 5 Microphotograph of VCO chip

method. The VCO chip was directly stuck onto the testing board with silver filled electro-conductive resin. Except for some bypass and decoupled capacitors, no other external components were needed. The VCO was tested by Agilent Performance Spectrum Analyzer E4440A. The output spectra were saved through floppy disk, shown in Fig. 6. From the marker in Fig. 6(a), we know that the oscillating frequency is 4.525GHz and the output power is 0.921dBm at $V_{TUNE} = 2.6\text{V}$. From the delta-mode marker in Fig. 6(b) we have



(a)



(b)

Fig. 6 Output spectra at $V_{TUNE} = 2.6\text{V}$ (a) Frequency and power marker; (b) Delta-mode marker

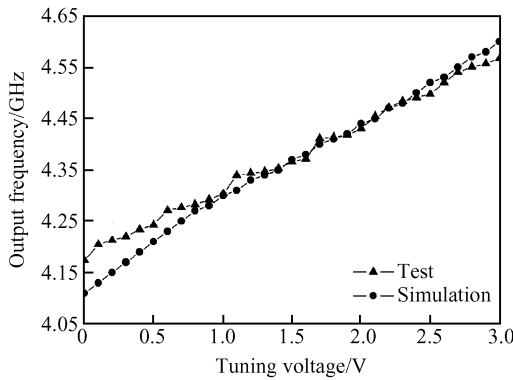


Fig. 7 Comparison of test and simulation of the frequency range

calculated the phase noise from Eq. (6), about $-112\text{dBc}/\text{Hz}@1\text{MHz}$.

$$L(f_{\text{offset}}) = 10\lg \frac{P_{\text{SSB}}}{P_s} = P_m + C_m - 10\lg \frac{B_m}{1\text{Hz}} - P_s \quad (6)$$

where $L(f_{\text{offset}})$ is the phase noise at offset frequency f_{offset} from the carrier (in dBc/Hz), B_m is the measurement bandwidth (in Hz), C_m is the calibration coefficient of the testing system (about $2\sim 3\text{dB}$), P_m is the noise power in measurement bandwidth (in dBm), and P_s is the signal power (in dBm). The measured phase noise is much worse than the simulated one mainly because of the fluctuation in the power supply of V_{CC} and V_{TUNE} , and also the radiation in testing board.

Figure 7 shows the comparison result of the measurement and simulated frequency tuning range, which shows very good consistency. It should be contributed to the use of air bridges. This time we not only used the inductor with structure of entire air bridge and air bridge post, but also used the air bridges to connect the paralleled tuning diodes. Thus the C_p in Eq. (4) was minimized to reduce the difference between simulation and measurement.

The VCO core dissipates 15.5mW from a 3.3V supply, and the output power is about 0dBm to 2dBm in the frequency tuning range. In order to make a fair comparison with other published 5GHz VCOs^[5~9,14,15], the figure of merit (FOM) for the VCO is calculated with the widely used FOM definition in Eq. (7), about $-173\text{dBc}/\text{Hz}$.

Table 1 Comparison of the FOM among the published 5GHz VCOs

Reference	Frequency /GHz	FOM /(dBc/Hz)	Tuning range/%
GaAs MESFET ^[5]	5.44	-168.6	12.9
CMOS ^[6]	5	-176.6	18
CMOS ^[7]	4.7	-173.1	4.3
SiGe ^[8]	5	-180.2	12.3
SiGe ^[9]	5.78	-169.7	3.5
InGaP HBT ^[14]	5.51	-165.3	8.0
InGaP HBT ^[15]	4.39	-179.6	6.8
This work	4.56	-173.2	8.9

$$\text{FOM} = L(f_{\text{offset}}) - 20\lg \frac{f_0}{f_{\text{offset}}} + 10\lg \frac{P_{\text{DC}}}{1\text{mW}} \quad (7)$$

Here, $L(f_{\text{offset}})$ is the measured phase noise from the oscillator frequency at frequency offset, f_{offset} . P_{DC} is the dc power consumption of the VCO. Table 1 shows the comparison of the phase noise figure of merit among some published 5GHz VCOs.

5 Conclusion

A fully-monolithic InGaP/GaAs HBT VCO for 5GHz wireless applications was presented. Although the tuning range of on-chip varactor is smaller than that of external varactor, the designed VCO using on-chip varactor covers the desired frequency range of 300MHz . And the measurement frequency tuning range is very close to the simulation one. The tuning range is 8.9% , and the FOM of the VCO is $-173.2\text{dBc}/\text{Hz}$.

References

- [1] Lee Thomas H. The design of CMOS radio-frequency integrated circuits. Cambridge; Cambridge University Press, 1998;12
- [2] Wang Fanglin, Yi Xiaofeng, Cui Fuliang, et al. A CMOS bluetooth wireless transmitter. Chinese Journal of Semiconductors, 2004, 25(4): 1030 (in Chinese) [王方林, 衣晓峰, 崔福良, 等. 一种 CMOS 蓝牙无线发送器电路. 半导体学报, 2004, 25(4): 1030]
- [3] Xu Qiming, Shi Yin, Gao Peng, et al. A DC-offset cancellation scheme in a direct-conversion receiver for IEEE 802.11a WLAN. Chinese Journal of Semiconductors, 2006, 27(4): 653
- [4] Tang Lu, Wang Zhigong, Huang Ting, et al. Design of a monolithic CMOS LC-voltage controlled oscillator with low phase noise for 4GHz frequency synthesizers. Chinese Journal of Semiconductors, 2006, 27(3): 459
- [5] Yoon S W, Park E C, Lee C H, et al. $5\sim 6\text{GHz}$ -band GaAs MESFET-based cross-coupled differential oscillator MMIC's

- with low phase-noise performance. IEEE Microw Wireless Compon Lett, 2001, 11(12):495
- [6] Samori C, Levantino S, Bocuzzi V. A -94 dBc/Hz @ 100 kHz, fully-integrated, 5-GHz, CMOS VCO with 18% tuning range for bluetooth applications. Proc IEEE Custom Integrated Circuits Conf, 2001:201
- [7] Kinget P. A fully integrated 2.7V 0.35 μ m CMOS VCO for 5GHz wireless applications. ISSCC Dig Tech Papers, 1998:226
- [8] Plouchart J O, Ainspan H, Soyuer M, et al. A fully-monolithic SiGe differential voltage-controlled oscillator for 5GHz wireless applications. Proc IEEE Radio Frequency IC Symp, 2000:57
- [9] Grau G, Langmann U, Winkler W, et al. A current-folded up-conversion mixer and VCO with center-tapped inductor in a SiGe-HBT technology for 5-GHz wireless LAN applications. IEEE J Solid-State Circuits, 2000, 35(9):1345
- [10] MacPherson S D. High frequency oscillator design using the technique of negative resistance. IEEE Africon 5th Africon Conference in Africa, 1999:1111
- [11] Rohde Ulrich L, Newkirk David P. RF/microwave circuit design for wireless applications. New York: John Wiley & Sons, Inc, 2000:769
- [12] Leeson D B. A simple model of feedback oscillator noise spectrum. Proc IEEE, 1966, 54(2):329
- [13] Razavi B. RF microelectronics. Prentice Hall, 1998:225
- [14] Yu S A, Meng C C, Lu S S. A 5.7GHz interpolative VCO using InGaP/GaAs HBT technology. IEEE Microw Wireless Compon Lett, 2002, 12(2):37
- [15] Eo Y, Kim K, Oh B. Low noise 5GHz differential VCO using InGaP/GaAs HBT technology. IEEE Microw Wireless Compon Lett, 2003, 13(7):259

面向 5GHz 无线应用的单片 InGaP/GaAs HBT 压控振荡器*

陈立强[†] 张 健 李志强 陈普锋 张海英

(中国科学院微电子研究所, 北京 100029)

摘要: 介绍了一种由商用 InGaP/GaAs 异质结双极晶体管工艺制成、基于负阻原理的单片压控振荡器, 此电路定位于 5GHz 频段下的无线应用. 在实际使用中, 除了旁路和去耦电容外, 无需外接其他外部元件. 测试得到的输出频率范围超过 300MHz, 为 4.17~4.56GHz, 与仿真结果非常吻合; 相位噪声为 -112 dBc/Hz@1MHz; 在 3.3V 电源电压下, 其核心部分的直流功耗为 15.5mW, 输出功率为 0~2dBm. 为了与其他振荡器比较, 还通过计算得到了相位噪声优值, 约为 -173.2 dBc/Hz. 同时, 还讨论了负阻振荡器的原理和设计方法.

关键词: 压控振荡器; 单片微波集成电路; 无线通信; InGaP/GaAs 异质结双极晶体管

EEACC: 1130B; 1230B

中图分类号: TN752.5

文献标识码: A

文章编号: 0253-4177(2007)06-0823-06

* 国家自然科学基金(批准号:60276021)和国家重点基础研究发展规划(批准号: G2002CB311901)资助项目

[†] 通信作者. Email: chenliqiang@ime.ac.cn

2006-12-25 收到, 2007-01-22 定稿